Purinergic signaling in the pulmonary neuroepithelial body microenvironment unraveled by live cell imaging

Ian De Proost,*,† Isabel Pintelon,* William J. Wilkinson,† Sofie Goethals,* Inge Brouns,* Luc Van Nassauw,* Daniela Riccardi,† Jean-Pierre Timmermans,* Paul J. Kemp,† and Dirk Adriaensen*,[1]

*Laboratory of Cell Biology and Histology, Department of Veterinary Sciences, University of Antwerp, Antwerp, Belgium; and †Cardiff School of Biosciences, Cardiff University, Museum Avenue, Cardiff, UK

ABSTRACT **Pulmonary neuroepithelial bodies (NEBs) are densely innervated groups of complex sensory airway receptors involved in the regulation of breathing. Together with their surrounding Clara-like cells, they exhibit stem cell potential through their capacity to regenerate depopulated areas of the epithelium following lung injury. We have employed confocal live cell imaging microscopy and novel electrophysiological techniques in a new *ex vivo* lung slice model to unravel potential purinergic signaling pathways within the NEB microenvironment. Quinacrine histochemistry indicated high amounts of vesicular ATP in NEB cells. Using a "reporter-patching" method adapted to create a uniquely sensitive and selective biosensor for the direct detection of ATP release from NEBs *ex vivo*, we demonstrated quantal ATP release from NEBs following their depolarization. Enhancing enzymatic extracellular ATP hydrolysis or inhibiting P2 receptors confirmed the central role of ATP in paracrine interactions between NEB cells and Clara-like cells. Combined calcium imaging, pharmacology, and immunohistochemistry showed that ligand-binding to functional $P2Y_2$ receptors underpins the activation of Clara-like cells. Hence, NEB cells communicate with their cellular neighbors in the NEB microenvironment by releasing ATP, which rapidly evokes purinergic activation of surrounding Clara-like cells. Besides ATP acting on the $P2X_3$ receptor expressing vagal sensory nerve terminals between NEB cells, local paracrine purinergic signaling within this potential stem cell niche may be important to both normal airway function, airway epithelial regeneration after injury, and/or the pathogenesis of small cell lung carcinomas.—De Proost, I., Pintelon, I., Wilkinson, W. J., Goethals, S., Brouns, I., Van Nassauw, L., Riccardi, D., Timmermans, J.-P., Kemp, P. J., Adriaensen, D. Purinergic signaling in the pulmonary neuroepithelial body microenvironment unraveled by live cell imaging. *FASEB J.* 23, 1153–1160 (2009)**

Key Words: ATP · NEB · Clara-like cells · mouse · lung

Clara-like cells, also referred to as variant Clara cell secretory protein expressing cells, represent a rare type of nonciliated epithelial cell present in the intrapulmonary airways of various animal species. Clara-like cells can be discriminated from the abundant common Clara cells by their resistance to naphthalene toxicity (1–3) and their invariable close association with pulmonary neuroepithelial bodies (NEBs; refs. 4, 5). NEBs are clusters of pulmonary neuroendocrine cells, which are widely distributed within the intrapulmonary airways. They show an extensive and selective innervation and contain various bioactive substances, *e.g.*, monoamine, peptide, and purine transmitters, within cytoplasmic dense-cored secretory granules (6–10). Clara-like cells reside exclusively around and over NEBs, shielding them almost completely from the airway lumen in many species, including humans and mice (11–15), with the result that only thin apical processes of NEB cells reach from the NEB microenvironment into the airway lumen.

NEBs have been suggested to have several functions in the regulation of physiological processes in the lungs during prenatal, perinatal, and postnatal life (reviews: refs. 7, 9, 10, 16–18), but the strongest evidence to date implicates them in airway oxygen sensing (reviews: refs. 16, 17, 19). Thus, native NEB cells and their immortalized cellular counterparts, H146 cells, detect a change in oxygen *via* substrate-delimited regulation of NADPH oxidase activity (20, 21). During hypoxia, a reduction in NADPH oxidase-dependent generation of H_2O_2 results in closure of specific oxygen-sensitive potassium channels (22–24) and, in native NEB cells at least, voltage-dependent serotonin release (25). In addition, pulmonary NEB cells are generally believed to be progenitor cells of the very aggressive small cell lung carcinomas (18), while Clara-like cells appear to be involved in airway epithelial regeneration following lung injury and exhibit many features of pluripotent stem cells (1–4, 26).

ATP is a well-known cotransmitter with classical neu-

[1] Correspondence: Laboratory of Cell Biology and Histology, Department of Veterinary Sciences, University of Antwerp, Groenenborgerlaan 171, B-2020 Antwerp, Belgium. E-mail: dirk.adriaensen@ua.ac.be

doi: 10.1096/fj.08-109579

rotransmitters in both the peripheral and central nervous system and is a powerful extracellular messenger to numerous non-neuronal cells (27, 28). Purinergic signaling is dependent on ligand binding to specific, membrane-bound receptors. These belong to one of the two purinoceptor families, P1 and P2. These two families are distinguished based on their distinct affinities for adenosine and ATP/ADP, respectively (29). Two main classes of P2 purinoreceptors are P2X and P2Y receptors (30). P2X receptors are ligand-gated cation channels, which facilitate Ca^{2+} influx during ligand binding, while P2Y receptors are G-protein coupled receptors that link ligand binding to release of Ca^{2+} from intracellular stores (31).

Although purinergic signaling within the NEB microenvironment has never been directly demonstrated, studies by us have shown that ATP accumulates in secretory vesicles of rat NEBs (32) and that rat and mouse NEBs are selectively contacted by $P2X_3$ receptor expressing vagal afferents (32, 33). Furthermore, using our recently developed *ex vivo* mouse lung slice NEB cell imaging model, we have shown that a depolarizing stimulus evokes Ca^{2+} influx into NEB cells, which is followed by a rise in intracellular free calcium ($[Ca^{2+}]_i$) in the surrounding Clara-like cells (34). Based on the consistent delay time between the initiation of the response in NEB cells and the subsequent response in the Clara-like cells, we hypothesized that indirect activation of the Clara-like cells may be induced by neurotransmitters released from the activated NEBs (34). To understand the potential interaction between NEBs and Clara-like cells in this putative lung stem cell niche, we have used live cell imaging in *ex vivo* lung slices to test the hypothesis that ATP is a paracrine transmitter in the NEB cell microenvironment. To this end, we have employed Ca^{2+} imaging to define the spatiotemporal cell-specific $[Ca^{2+}]_i$ changes, and pharmacology and immunohistochemistry to identify and localize ATP receptors in cells of the niche. Furthermore, we have developed the use of a voltage-clamped reporter cell line [human embryonic kidney (HEK) 293 cells stably expressing rat $P2X_2$ receptors] to detect real-time release of ATP from identified cells within the lung slice. Using this "reporter-patching" ATP biosensor technique, we provide conclusive and direct evidence that ATP is released by NEBs in response to depolarization in lung slices.

MATERIALS AND METHODS

Animals

Lung tissue was obtained from 5- to 18-day-old C57-Bl6 mice (n=34; Janvier, Bio Services, Uden, The Netherlands). All animals were housed with their mothers in acrylic cages in an acclimatized room (12:12 h light-dark cycle; 22±3°C) and were provided with water and food *ad libitum*. National and European principles of laboratory animal care were followed, and experiments were approved by the animal ethics committee of the University of Antwerp.

All animals were killed by intraperitoneal injection of an overdose of sodium pentobarbital (Nembutal 200 mg/kg, CEVA Santé Animale, Brussels, Belgium) containing heparin (500 U/kg; Rhône Poulenc Rorer 256S68F12, Brussels, Belgium).

Drugs, solutions, and perfusion

A standard physiological solution was used throughout the various experiments, containing (in mM): 130 NaCl, 5 KCl, 1.2 $CaCl_2{\cdot}2H_2O$, 1 $MgSO_4{\cdot}7H_2O$, 11 D-glucose, 20 HEPES, pH 7.42, adjusted with NaOH. The osmolarity of all solutions was maintained between 285 and 300 mosM. Solutions containing high extracellular potassium ($[K^+]_o$) were prepared by adding KCl to the desired concentration, while NaCl was adjusted accordingly. For Ca^{2+}-free solution, $CaCl_2{\cdot}2H_2O$ was replaced by 1 mM ethylenediamine tetraacetic acid disodium salt dihydrate (EDTA).

All chemicals and drugs that are not specifically referred to were purchased from Sigma (Bornem, Belgium), except for UTPγS (Jena Bioscience, Jena, Germany), and Fluo-4 acetoxymethylester (Fluo-4 AM; F14201) and 4-(4-diethylaminostryryl)-*N*-methylpyridinium iodide (4-Di-2-ASP; D-289), which were provided by Molecular Probes (Invitrogen, Merelbeke, Belgium). All stimuli were applied to lung slices that were submerged in a tissue bath (2 ml) mounted on the microscope stage, perfused by a gravity-fed system (flow rate of >5 ml/min) with electrically triggered valves that allowed the fast and reproducible exchange of solutions. The $P2X_2$ reporter-patching experiments were an exception to this protocol (see below and Supplemental Data, SF Materials and Methods).

Preparation of lung slices and staining of neuroepithelial bodies

Vibratome slices were cut from lung lobes and stained for NEBs using 4-Di-2-ASP as previously published (34, 35). In short, lung tissue was stabilized by instillation of a 2% agarose solution (low-melt agarose, A4018, Sigma). Lung slices were cut using a vibratome (HM650 V; Microm International, Walldorf, Germany) and subsequently incubated for 4 min with 4 μM 4-Di-2-ASP in Dulbecco's modified Eagle's medium/F-12 (DMEM-F-12; Life Technologies, Inc., Invitrogen) at 37°C, rinsed, and kept in DMEM-F-12 in an incubator (37°C; 5% CO_2/95% air) for further use within 12 h of sacrificing the animal. For reporter-patching experiments (see below), lung slices were made using an Integraslice vibratome (7550 PSDS; Campden Instruments, Leicester, UK).

Ca^{2+} indicator loading procedure

Lung slices stained with 4-Di-2-ASP were incubated in physiological solution with 10 μM Fluo-4 AM, 100 μM sulfobromophtalein, 0.1% dimethyl sulfoxide, and 0.02% Pluronic F-127 for 1 h at 22°C. The slices were subsequently washed (10 min; 22°C) in physiological solution to allow for complete deesterification of intracellular Fluo-4 AM.

Quinacrine loading of mouse lung slices

Freshly cut lung slices were incubated for 2 h in 1 μM quinacrine (Mepacrine; Q3251; Sigma) in DMEM-F-12 (37°C) and rinsed in DMEM-F-12 (10 min; 37°C). Quinacrine accumulation was imaged in the live lung slices using an Olympus DP70 digital camera system (Olympus, Tokyo, Japan) on an epifluorescence microscope (see below). Subsequently, the slices were fixed (3 h) with 4% paraformaldehyde (4% PF; 0.1 M phosphate buffer, pH 7.4) and further processed for immunohistochemical staining (see below).

Immunohistochemical staining of lung slices and cryosections

For immunohistochemical staining, freshly cut lung slices were fixed (4% PF) for 3 h. For cryosectioning, lungs were transcardially perfused with the standard physiological salt solution and subsequently filled with 4% paraformaldehyde (0.1 M phosphate buffer, pH 7.4) *via* the trachea. Lungs, trachea, esophagus, and heart were dissected *en bloc*, degassed, and further immersion-fixed for 30 min. After rinsing in PBS, tissues were stored overnight in 20% sucrose (in PBS; 4°C), and mounted in Tissue Tek (Sakura Finetek Europe, Zoeterwoude, The Netherlands). Cryostat sections (30 μm thickness) of the whole blocs were thaw-mounted on poly-L-lysine-coated microscope slides, dried at 37°C (2 h).

Immunocytochemical incubations were performed in a closed, humidified container (22°C). All primary and secondary antisera were diluted in phosphate-buffered saline (PBS; 0.01 M, pH7.4) containing 10% normal goat serum, 0.1% bovine serum albumin, 0.05% thimerosal, and 0.01% NaN_3 (PBS*). Prior to incubation with the primary antisera, specimens were kept in PBS* containing 1% Triton-X-100 (1 h for slices, 30 min for cryostat sections). Sections were then incubated overnight with one of the following rabbit polyclonal primary antibodies: protein gene-product 9.5 (PGP9.5; 1:500; AB1761; Chemicon, Temecula, CA, USA) or calcitonin gene-related peptide (CGRP; 1:500; C8198; Sigma), as NEB markers; urine protein 1 (UP1; 1:200; A0257; Dakocytomation, Glostrup, Denmark), a Clara cell-specific protein; $P2Y_2$ receptor (1:200; APR-010; Alomone, Jerusalem, Israel). To visualize immunoreactivity, sections were further incubated (3 h for slices, 2 h for cryostat sections) with Fab fragments of goat anti-rabbit immunoglobulins conjugated with Cy3 (GAR-Fab-Cy3; 1:2000; 111-167-003, Jackson ImmunoResearch, West Grove, PA, USA) or with FITC (GAR-Fab-FITC; 1:100; 111-097-003; Jackson ImmunoResearch). To allow for double labeling with a second primary antibody raised in rabbit ($P2Y_2$-PGP9.5 or UP1-PGP9.5), the sections were incubated for 6 h with unconjugated Fab fragments of goat anti-rabbit immunoglobulins (GAR-Fab; 1:50; 111-007-003; Jackson ImmunoResearch) in between the two incubations. After a final wash in PBS, the sections were mounted in Citifluor (19470; Ted Pella, Redding, CA, USA).

Control experiments for the immunohistochemical procedures

To determine the level of nonspecific staining, negative staining controls for all immunohistochemical procedures were performed by substitution of nonimmune sera for the primary or secondary antisera. Specificity of the $P2Y_2$ antibody was tested by preabsorption of the antiserum with the corresponding antigen (1 μg peptide/μg antibody; 1 h; P41232; Alomone,) prior to incubation of the tissue with the antibody. To check for possible cross-reactivity after consecutive multiple staining using two primary antisera raised in the same species, the results of single immunostaining for the different antisera were evaluated and compared with those of multiple labeling experiments.

Microscopic data acquisition

An epifluorescence microscope (Zeiss Axiophot; Carl Zeiss, Jena, Germany) equipped with filters for the visualization of FITC (Zeiss 17; BP 485–520/FT 510/BP 515–565), Cy3 (Zeiss 00; BP530–585/FT 600/LP 615), and Quinacrine (Zeiss 18; BP 390–420/FT 425/LP 450) was used to evaluate the immunostaining results and to image quinacrine accumulation in lung slices. An inverted microscope (Zeiss Axiovert 200; Carl Zeiss), attached to a microlens-enhanced dual spinning disk confocal system (Ultra*VIEW* ERS; PerkinElmer, Seer Green, UK), equipped with a three-line (488, 568, and 647 nm) argon-krypton laser for excitation of the FITC and Cy3 labels was used for all confocal imaging. For the physiological live cell imaging experiments, lung slices were transferred to a perfusion chamber on the microscope stage and were restrained with a golden ring spanned with a sheet of nylon mesh.

Data analysis

Time-lapse recordings were analyzed offline using Volocity 3 software (Improvision, Coventry, UK). For analysis, individual images were studied as gray value datasets. Regions of interest (ROIs) were drawn manually around identified cells of interest. For every ROI, the fluorescence intensity expressed as arbitrary units (A.U.) was plotted against time. To facilitate interpretation of the results, gray values were adjusted for the basal level of fluorescence that was present at the start of imaging. All fluorescence values presented are relative. The shown graphs are representative for multiple experiments performed under the respective conditions.

Direct detection of ATP release: reporter patching

A reporter-patching method was adapted for use in lung slices from a method originally designated as the "sniffer-patch" technique for measuring GABA release from neurons (36). This reporter-patching method allowed for creating a uniquely sensitive and selective biosensor for the direct detection of ATP release from NEBs in *ex vivo* lung slices. HEK 293 cells stably heterologously expressing the recombinant rat $P2X_2$ purinoceptor ($rP2X_2$) were a kind gift of Prof. R. A. North (University of Manchester, Manchester, UK). NEBs were localized in 4-Di-2-ASP-stained lung slices. Single HEK 293 cells expressing $rP2X_2$ purinoceptors were voltage-clamped at −60 mV in the whole-cell configuration and gently manipulated to within a few micrometers of the NEB in the slice. Following a period of baseline recording, a 10 s pulse of high K^+ solution was applied to the NEB using a multibarreled, rapid solution changing system (RSC; Intracel, Royston, UK), and ATP release was detected as short inward current spikes. For detailed description of the ATP biosensor reporter-patching experiments, see Supplemental Data, SF Materials and Methods.

RESULTS

Quinacrine accumulation in pulmonary neuroepithelial bodies

Quinacrine was seen to accumulate in intraepithelial cell groups, reminiscent of NEBs, at all levels of the intrapulmonary airways in mouse lung slices (**Fig. 1*A***). Subsequent immunohistochemical staining of these slices with antibodies against PGP9.5 or CGRP, for the unambiguous identification of NEB cells, confirmed that the intraepithelial quinacrine-labeled cell groups invariably corresponded to pulmonary NEBs (Fig. 1*B*; Supplemental Fig. 7).

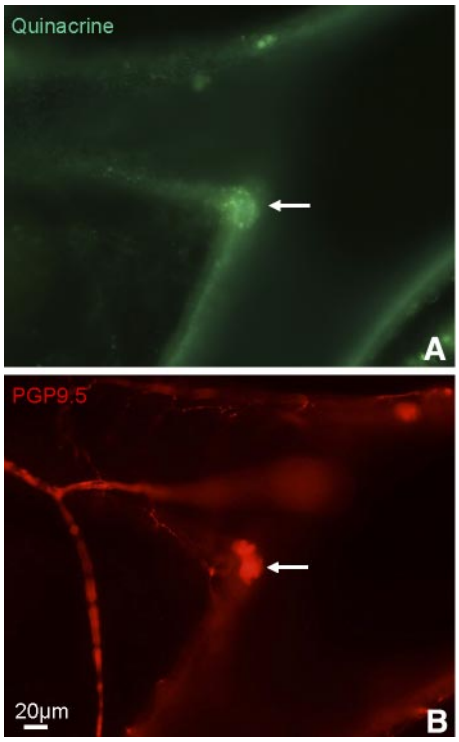

Figure 1. Quinacrine fluorescence (cyan) (*A*) colocalizes with protein gene-product 9.5 (PGP9.5) immunostaining (red, Cy3 fluorescence) (*B*) in a cell group located within the epithelium at a branching point of an airway (arrows), indicative of vesicular ATP accumulation in an NEB. See Supplemental Fig. 7 for additional higher magnification images.

ATP evokes rises in intracellular free Ca^{2+} in Clara-like cells, but not in neuroepithelial bodies

Short-term stimulation of 4-Di-2-ASP-stained (**Fig. 2*Bi***) and Fluo-4 loaded lung slices with ATP (10 μM, 10 s) evoked an increase in cytoplasmic Fluo-4 fluorescence, indicative of a rise in $[Ca^{2+}]_i$, in Clara-like cells, Clara cells, and to a lesser extent in ciliated cells, but never in NEB cells (Fig. 2*A*, *Bii, iii*; Supplemental Video 1*A*). Subsequent stimulation of the lung slice with the established positive control (50 mM $[K^+]_o$; 5 s), resulted in a rise in $[Ca^{2+}]_i$ in all NEBs, confirming the appropriate Fluo-4 loading and viability of the NEB cells and the typical activation of surrounding Clara-like cells after a 1–2 s delay (Fig. 2*A*, *Biv–vi*; Supplemental Video 1*B*). An extensive description of the unique possibilities of this model and the criteria that are used to differentiate among the different airway epithelial cell types in live lung slices was recently published (34) (also see Supplemental Fig. 8). In short, incubation of lung slices with 4-Di-2-ASP results in a mosaic of polygonal fluorescent epithelial cells, intermingled with almost nonfluorescent rounded cells. Sequential time-lapse imaging of 4-Di-2-ASP fluorescence and transmitted light images identified the 4-Di-2-ASP fluorescent cells as ciliated epithelial cells that showed beating cilia. The nonfluorescent, nonciliated cells were found to correspond to Clara cells. Scattered in the airway epithelium, conspicuous 4-Di-2-ASP fluorescent clusters of small, rounded epithelial cells could be identified as pulmonary NEBs, as was confirmed by immunohistochemical staining (ref. 35; Supplemental Fig. 8). The NEB cells were found to be typically surrounded by a continuous layer of nonfluorescent Clara cells, the so-called Clara-like cells. This indisputable identification method in combination with calcium imaging experiments allowed us to reliably identify the different airway epithelial cells that responded to ATP and its analogues in the present study.

ATP is involved in the activation of Clara-like cells on depolarization of neuroepithelial bodies with high extracellular K^+

Most of the Clara-like cells that revealed an increase in $[Ca^{2+}]_i$ to an initial high $[K^+]_o$ stimulus also displayed a second activation after renewed stimulation with high $[K^+]_o$ following 5 min of rinsing with the standard physiological solution (n=45/48, 94%; **Fig. 3*A***). This proportion was reduced significantly to 57% (n=25/44) when apyrase (2 U/ml) and adenosine deaminase (2 U/ml), two enzymes that together break down extracellular ATP to inosine, were added to the perfusion solution (Fig. 3*B*). Using suramin (100 μM), a nonselective

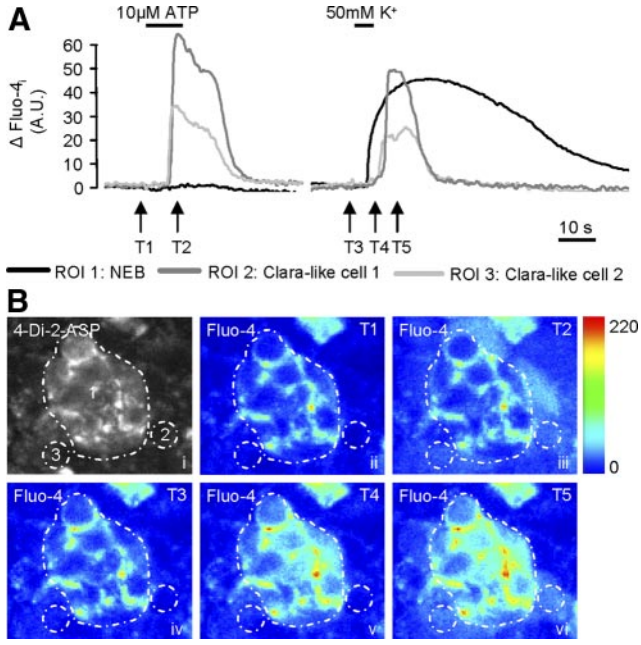

Figure 2. *A*) Representative time course of changes in Fluo-4 fluorescence intensity (ΔFluo-4_i) measured in NEB cells and surrounding Clara-like cells in a 4-Di-2-ASP-stained lung slice during sequential challenges with 10 μM ATP and high $[K^+]_o$. Traces were obtained from the ROI marked on the fluorescence images in *B*: ROI 1, NEB; ROI 2, Clara-like cell 1; ROI 3, Clara-like cell 2. *B)* Fluorescence images showing 4-Di-2-ASP signal (NEB cell staining) (*i*) and pseudocolor time-lapse images of Fluo-4 (*ii–vi*) in the NEB and surrounding epithelial cells at different time points, during the ATP (T1 and T2) and high $[K^+]_o$ (T3–T5) applications. Color-coded intensity calibration bar is shown at right. Corresponding time-lapse recordings are shown in Supplemental Video 1*A*, *B*.

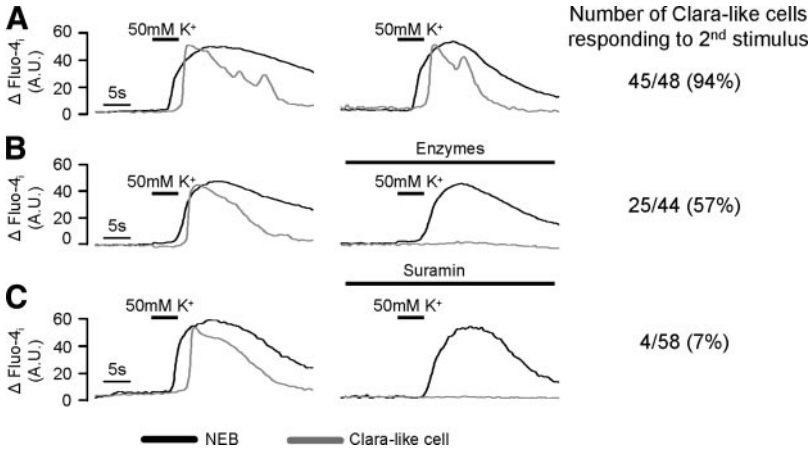

Figure 3. Exemplar time courses of changes in Fluo-4 fluorescence intensity of NEBs and Clara-like cells. A paired stimulus protocol was used in which the first stimulus was high $[K^+]_o$ alone and the second stimulus was either high $[K^+]_o$ alone (*A*), high $[K^+]_o$ in the presence of apyrase (2 U/ml) and adenosine deaminase (2 U/ml) (*B*), or high $[K^+]_o$ in the presence of 100μM suramin (*C*). Proportion and percentage of cells responding to the second stimulus are shown to the right of each trace.

blocker of purinoceptors, only 7% (n=4/58) of the Clara-like cells reacted to a second stimulation with high $[K^+]_o$ (Fig. 3*C*).

Clara-like cells express functional P2Y receptors

The role of purinoceptors in the activation of Clara-like cells was demonstrated by an almost complete blockade (n=63/66) of the ATP response in the presence of 100 μM suramin (**Fig. 4*A***). In the absence of extracellular Ca^{2+}, application of ATP (10 μM) evoked a rise in $[Ca^{2+}]_i$ in almost all Clara-like cells (34/35, Fig. 4*B*), suggesting exclusive functional expression of P2Y receptors. This notion was strengthened by the observations that phospholipase C inhibition with the irreversible antagonist U-73122 (10 μM) blocked the ATP evoked $[Ca^{2+}]_i$ rise in all Clara-like cells (n=45/45; Fig. 4*C*) and that U-73343 (10 μM), the inactive analog of U-73122, was without effect (Fig. 4*D*). Furthermore, responses of Clara-like cells to the application of different ATP analogues (10 μM) allowed pharmacological definition of the P2Y receptor class that was involved (**Fig. 5*A–G***). Thus, the rank order of potency was UTPγS= ATPγS>UTP≫2MeSATP>ADP=UDP=α,β-MeATP, which suggests functional expression of $P2Y_2$ receptors, an idea fully supported by immunolocalization (Fig. 5*H*).

Using $P2X_2$ reporter patching to detect quantal ATP release from neuroepithelial bodies

The experimental protocol that was used to directly detect the release of ATP from pulmonary NEBs is illustrated in **Figs. 6*Ai–iii***. Patched HEK 293 cells, expressing $rP2X_2$ receptors, were gently manipulated into positions as close as possible to the airway epithelium just downstream of NEBs. A 2 s pulse of 10 μM ATP was applied as a positive control. Following the demonstration that the HEK 293 cell could respond to ATP, a 10 s pulse of high $[K^+]_o$ solution was applied to the NEB. ATP release was detected within ~1 s as discrete inward current spikes for the duration of the NEB depolarizing protocol (Fig. 6*Bi*). These currents had temporal characteristics (Fig. 6*Bii*) very similar to those reported as quantal transmitter release detected by polarized carbon fiber amperometry in other systems (*e.g.*, see ref. 37). The high $[K^+]_o$ solution never elicited inward current spikes when the cell was moved away from the NEB (not shown). However, high $[K^+]_o$ did produce a rapid liquid junction potential, which allowed us to estimate the time lag between solution exchange and ATP detection. This was typically in the order of 1 s and in agreement with estimations from the Ca^{2+} imaging experiments (see Fig. 2*A*).

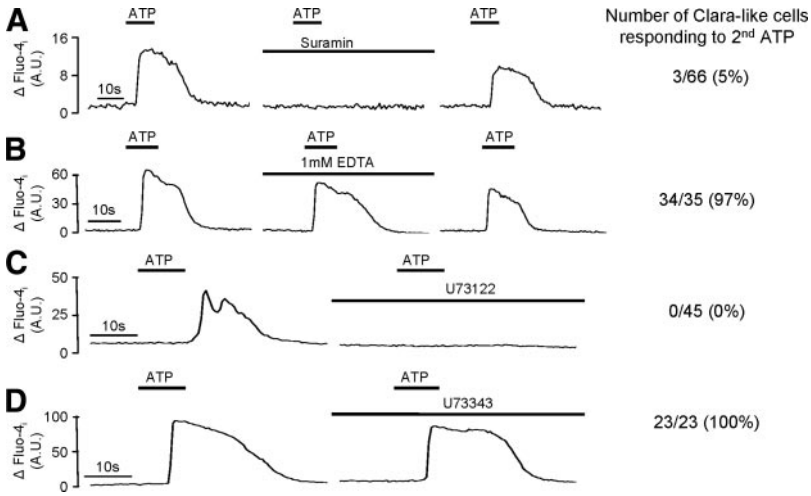

Figure 4. Exemplar time courses of changes in Fluo-4 fluorescence intensity of Clara-like cells. A paired or triple stimulus protocol was used in which the first and third stimuli were 10 μM ATP alone and the second stimulus was either 10 μM ATP in the presence of 100 μM suramin (*A*), 10 μM ATP in the nominal absence of extracellular Ca^{2+} (*B*), 10 μM ATP in the presence of 10 μM U-73122 (*C*) or 10 μM ATP in the presence of 10μM U-73343 (*D*). Proportion and percentage of cells responding to the second stimulus are shown to the right of each trace.

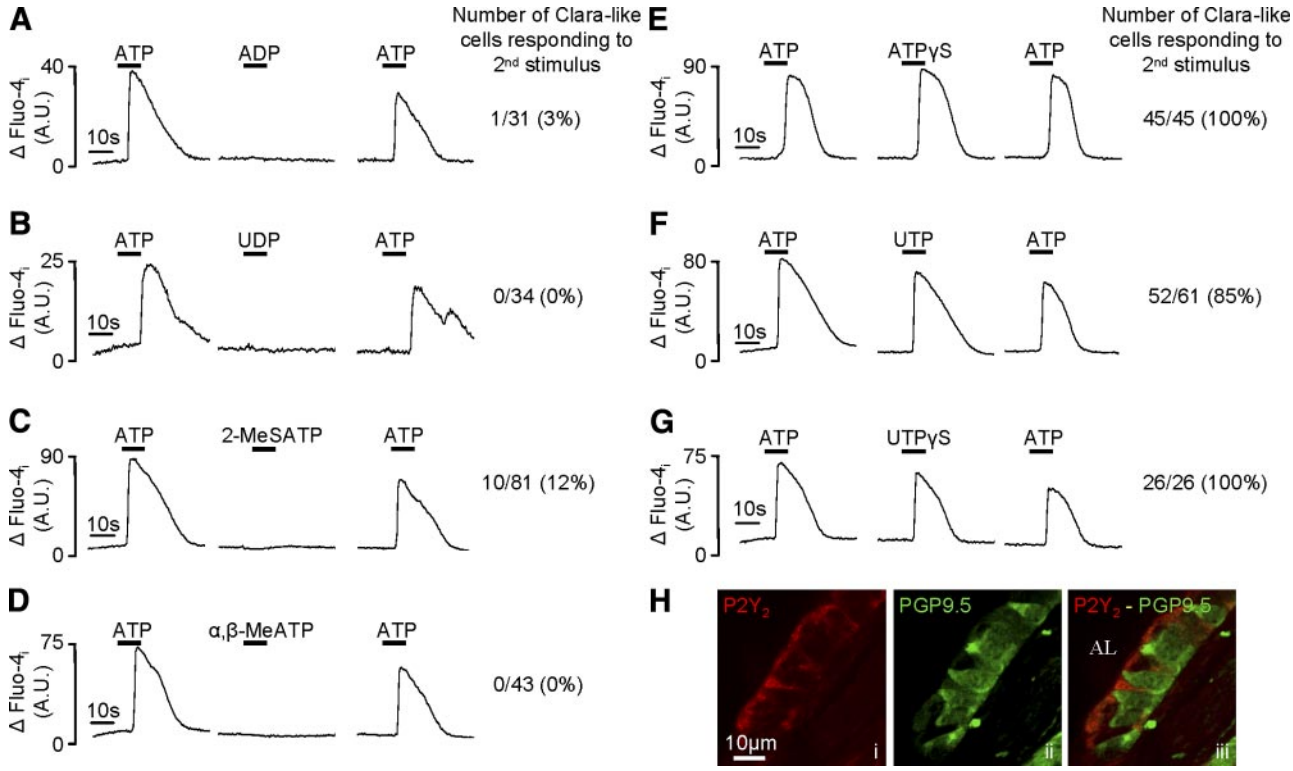

Figure 5. Exemplar time courses of changes in Fluo-4 fluorescence intensity of Clara-like cells. *A–G*) A triple stimulus protocol was used in which the first and third stimuli were 10 μM ATP alone and the second stimulus was 10 μM of either ADP (*A*), UDP (*B*), 2-MeSATP (*C*), α,β-MeATP (*D*), ATPγS (*E*), UTP (*F*), or UTPγS (*G*). Proportion and percentage of cells responding to the second stimulus are shown to the right of each trace. *H*) Immunohistochemical double-labeling for $P2Y_2$ receptors (red, Cy3 fluorescence) (*i*), PGP9.5 (green, FITC fluorescence) (*ii*), and overlay (*iii*). Note that the PGP9.5-immunoreactive NEB cells are shielded from the airway lumen by $P2Y_2$ expressing Clara-like cells. Several NEB cells show a thin apical process that seems to reach the luminal surface of the airway in this section. AL, airway lumen.

DISCUSSION

This study establishes a functional coupling between NEB cells and Clara-like cells in the stem cell niche of the NEB microenvironment. Thus, depolarization of pulmonary NEB cells evokes Ca^{2+}-mediated quantal ATP release followed by activation of the surrounding Clara-like cells *via* ligand binding at $P2Y_2$ purinoceptors.

Quinacrine accumulation shows that mouse NEBs store vesicular ATP, similar to what has been reported for rat NEBs (32) and other neurosecretory cells (38). More dramatic and direct evidence that ATP is released by NEB cells is shown in Fig. 6. Here we have used reporter patching as a uniquely sensitive and selective ATP biosensor detection method. Similar protocols have been used to detect GABA release from single neurons (39) and ATP release from single cells (40–42) but have never been employed in an *ex vivo* tissue system as demonstrated herein. Using such reporter patching, we could detect quantal ATP release from

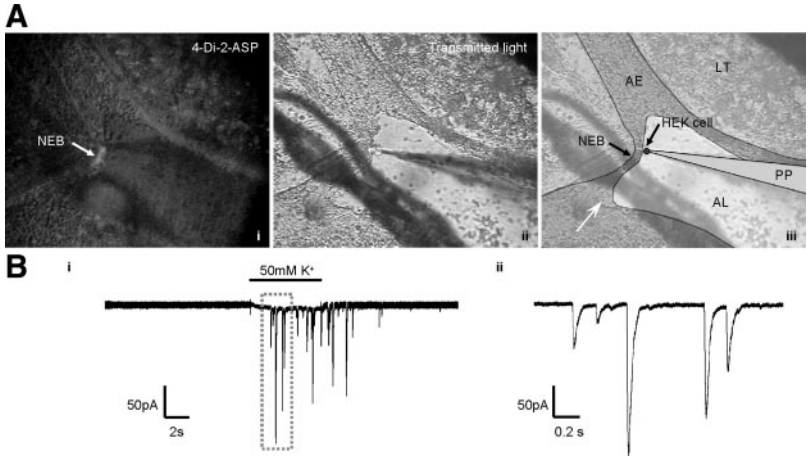

Figure 6. Representative recording of quantal ATP release from NEB cells in a lung slice, detected by reporter patching. *A*) 4-Di-2-ASP image to allow visualization of the NEB (*i*), brightfield image (*ii*), and cartoon overlay illustrating that the solution outflow (white arrow) is directly aligned with the NEB and the voltage-clamped, $rP2X_2$-expressing HEK 293 cell (*iii*). AE, airway epithelium; AL, airway lumen; LT, lung tissue; PP, patch pipette. *B*) Full-scale example of the ATP-evoked current (whole cell holding potential = −60 mV) (*i*), with spike characteristics shown on a faster time base (*ii*).

NEBs only when the patched HEK cell was in very close contact with the apical surface of the airway epithelium just downstream of the NEB/Clara-like cell complex. Moving the HEK cell even 10 μm away from the NEB resulted in failure to detect ATP release. These data lend further weight to the argument that NEB cells release ATP into their microenvironment only.

Notably, ATP released from NEBs produced paracrine activation of Clara-like cells. $P2Y_2$ was identified pharmacologically and immunohistochemically as the functional purinoreceptor involved. It is remarkable that only Clara-like cells respond to the ATP released from NEBs, while in agreement with airway epithelial cell culture studies (43, 44), we confirmed that Clara and ciliated cells can be activated by exogenously applied ATP. The latter strongly suggests that ATP released from the NEBs could activate ATP receptors only within the tightly sealed NEB microenvironment, which consists of NEB cells, intraepithelial nerve terminals, and Clara-like cells, but apparently is not able to reach other epithelial cells. To restrict the purinergic activation to the NEB microenvironment, and prevent disturbance of the other physiological ATP-mediated processes in surrounding cells or tissues, ATP is likely degraded by endogenous ectonucleotidases before significant quantities can "escape" from the closed environment.

In contrast to the Clara-like cells, NEBs were not activated by external application of any of the ATP analogues in mouse lung slices. Even αβ-MeATP, a very potent agonist for $P2X_3$ or $P2X_{2/3}$ receptors was ineffective in all NEBs studied. The latter is at variance with the results of Fu and colleagues (45), who used whole-cell patch clamp and amperometry of pulmonary NEBs in hamster lung slices and reported that ATP activates $P2X_{2/3}$ heteromeric receptors on the NEB cell membrane, resulting in the release of serotonin. At present, species-dependent differences seem to be the most plausible explanation.

However, a myelinated vagal nodose afferent nerve fiber population, expressing $P2X_3$ ATP receptors on the terminal arborizations, has been described to make selective intraepithelial contacts with NEB cells in rat (32) and mouse (33) lungs (Supplemental Fig. 9). The present evidence that activated NEB cells release ATP strengthens the suggestion that NEBs may also transduce sensory information toward the central nervous system *via* the $P2X_3$ expressing terminals of vagal afferents within the NEB microenvironment.

This study revealed that activation of NEB cells in *ex vivo* mouse lung slices evokes subsequent purinergic paracrine effects on the surrounding Clara-like cells by binding of released ATP to $P2Y_2$ receptors. Hence, besides ATP acting on the $P2X_3$ receptor expressing vagal sensory nerve terminals between NEB cells, our data reveal an unambiguous interaction between NEB cells and the shielding Clara-like cells. Considering the stem cell-like characteristics of Clara-like cells, this local purinergic signaling may be of great importance for normal airway function, for airway epithelial regeneration after injury and/or for the pathogenesis of small cell lung carcinomas. FJ

This work was supported by the following research grants: Fund for Scientific Research-Flanders (G.0085.04 and G.0081.08 to D.A.); NOI-BOF 2003 and GOA-BOF 2007 (to D.A.), and KP-BOF 2006 (to I.B.) from the University of Antwerp; BBSRC, BHF, and MRC grants (to D.R. and P.J.K.). We especially thank Profs. J.-M. Boeynaems and B. Robaye (Université Libre de Bruxelles, Brussels, Belgium) for the stimulating discussions about purinergic signaling. We thank J. Van Daele and D. De Rijck for help with microscopy, imaging and illustrations, and S. Kockelberg and H. De Pauw for administrative help.

REFERENCES

1. Reynolds, S. D., Giangreco, A., Power, J. H., and Stripp, B. R. (2000) Neuroepithelial bodies of pulmonary airways serve as a reservoir of progenitor cells capable of epithelial regeneration. *Am. J. Pathol.* **156,** 269–278
2. Bishop, A. E. (2004) Pulmonary epithelial stem cells. *Cell. Prolif.* **37,** 89–96
3. Hong, K. U., Reynolds, S. D., Giangreco, A., Hurley, C. M., and Stripp, B. R. (2001) Clara cell secretory protein-expressing cells of the airway neuroepithelial body microenvironment include a label-retaining subset and are critical for epithelial renewal after progenitor cell depletion. *Am. J. Respir. Cell Mol. Biol.* **24,** 671–681
4. Reynolds, S. D., Hong, K. U., Giangreco, A., Mango, G. W., Guron, C., Morimoto, Y., and Stripp, B. R. (2000) Conditional clara cell ablation reveals a self-renewing progenitor function of pulmonary neuroendocrine cells. *Am. J. Physiol. Lung Cell Mol. Physiol.* **278,** L1256–L1263
5. Lauweryns, J. M., and Peuskens, J. C. (1972) Neuro-epithelial bodies (neuroreceptor or secretory organs?) in human infant bronchial and bronchiolar epithelium. *Anat. Rec.* **172,** 471–481
6. Scheuermann, D. W. (1987) Morphology and cytochemistry of the endocrine epithelial system in the lung. *Int. Rev. Cytol.* **106,** 35–88
7. Adriaensen, D., and Scheuermann, D. W. (1993) Neuroendocrine cells and nerves of the lung. *Anat. Rec.* **236,** 70–85
8. Adriaensen, D., Brouns, I., Van Genechten, J., and Timmermans, J.-P. (2003) Functional morphology of pulmonary neuroepithelial bodies: extremely complex airway receptors. *Anat. Rec.* **270A,** 25–40
9. Sorokin, S. P., and Hoyt, R. F. (1989) Neuroepithelial bodies and solitary small-granule cells. In *Lung Cell Biology* (Massaro, D., ed) pp. 191–344, Marcel Dekker, New York, NY, USA
10. Adriaensen, D., Brouns, I., Pintelon, I., De Proost, I., and Timmermans, J.-P. (2006) Evidence for a role of neuroepithelial bodies as complex airway sensors: comparison with smooth muscle-associated airway receptors. *J. Appl. Physiol.* **101,** 960–970
11. Hung, K.-S. (1982) Development of neuroepithelial bodies in pre- and postnatal mouse lungs: scanning electron microscopic study. *Anat. Rec.* **203,** 285–291
12. Haller, C. J. (1994) A scanning and transmission electron microscopic study of the development of the surface structure of neuroepithelial bodies in the mouse lung. *Micron* **25,** 527–538
13. Pearsall, A. D., Hoyt, R. F., and Sorokin, S. P. (1985) Three-dimensional reconstruction of a small-granule paracrine cell cluster in an adult hamster bronchus. *Anat. Rec.* **212,** 132–142
14. De Proost, I., Brouns, I., Pintelon, I., Timmermans, J.-P., and Adriaensen, D. (2007) Pulmonary expression of voltage-gated calcium channels: special reference to sensory airway receptors. *Histochem. Cell Biol.* **128,** 301–316
15. Stahlman, M. T., and Gray, M. E. (1984) Ontogeny of neuroendocrine cells in human fetal lung. I. An electron microscopic study. *Lab. Invest.* **51,** 449–463
16. Kemp, P. J., Searle, G. J., Hartness, M. E., Lewis, A., Miller, P., Williams, S., Wootton, P., Adriaensen, D., and Peers, C. (2003) Acute oxygen sensing in cellular models: relevance to the

physiology of pulmonary neuroepithelial and carotid bodies. *Anat. Rec.* **270A,** 41–50
17. Cutz, E., and Jackson, A. (1999) Neuroepithelial bodies as airway oxygen sensors. *Respir. Physiol.* **115,** 201–214
18. Linnoila, R. I. (2006) Functional facets of the pulmonary neuroendocrine system. *Lab. Invest.* **86,** 425–444
19. Cutz, E., Fu, X. W., Yeger, H., Peers, C., Kemp, P. J. (2003) Oxygen sensing in pulmonary neuroepithelial bodies and related tumor cell models. In *Lung Oxygen Sensing* (Lahiri, S., Semenza, G. L., and Prabhakar, N. R., eds) pp. 567–602, Marcel Dekker, New York, NY, USA
20. Fu, X. W., Wang, D., Nurse, C. A., Dinauer, M. C., and Cutz, E. (2000) NADPH oxidase is an O_2 sensor in airway chemoreceptors: evidence from K^+ current modulation in wild-type and oxidase-deficient mice. *Proc. Natl. Acad. Sci. U. S. A.* **97,** 4374–4379
21. O'Kelly, I., Lewis, A., Peers, C., and Kemp, P. J. (2000) O_2 sensing by airway chemoreceptor-derived cells: protein kinase C activation reveals functional evidence for involvement of NADPH oxidase. *J. Biol. Chem.* **275,** 7684–7692
22. Youngson, C., Nurse, C., Yeger, H., and Cutz, E. (1993) Oxygen sensing in airway chemoreceptors. *Nature* **365,** 153–155
23. Wang, D., Youngson, C. R., Wong, V., Yeger, H., Dinauer, M. C., Vega-Saenz, M. E., Rudy, B., and Cutz, E. (1996) NADPH-oxidase and a hydrogen peroxide-sensitive K^+ channel may function as an oxygen sensor complex in airway chemoreceptors and small cell lung carcinoma cell lines. *Proc. Natl. Acad. Sci. U. S. A.* **93,** 13182–13187
24. O'Kelly, I., Stephens, R. H., Peers, C., and Kemp, P. J. (1999) Potential identification of the O_2-sensitive K^+ current in a human neuroepithelial body-derived cell line. *Am. J. Physiol.* **276,** L96–L104
25. Fu, X. W., Nurse, C. A., Wong, V., and Cutz, E. (2002) Hypoxia-induced secretion of serotonin from intact pulmonary neuroepithelial bodies in neonatal rabbit. *J. Physiol.* **539,** 503–510
26. Giangreco, A., Groot, K. R., and Janes, S. M. (2007) Lung cancer and lung stem cells: strange bedfellows? *Am. J. Respir. Crit. Care. Med.* **175,** 547–553
27. Burnstock, G., and Knight, G. E. (2004) Cellular distribution and functions of P2 receptor subtypes in different systems. *Int. Rev. Cytol.* **240,** 31–304
28. Burnstock, G. (2007) Purine and pyrimidine receptors. *Cell. Mol. Life Sci.* **64,** 1471–1483
29. Burnstock, G. (1978) A basis for distinguishing two types of purinergic receptor. In *Cell Membrane Receptors for Drugs and Hormones: A Multidisciplinary Approach* (Straub, R. W., and Bolis, L., eds) pp. 107–118, Raven Press, New York, NY, USA
30. Abbracchio, M. P., and Burnstock, G. (1994) Purinoceptors: are there families of P2X and P2Y purinoceptors? *Pharmacol. Ther.* **64,** 445–475
31. von Kügelgen, I., and Wetter, A. (2000) Molecular pharmacology of P2Y-receptors. *Naunyn. Schmiedebergs. Arch. Pharmacol.* **362,** 310–323
32. Brouns, I., Adriaensen, D., Burnstock, G., and Timmermans, J.-P. (2000) Intraepithelial vagal sensory nerve terminals in rat pulmonary neuroepithelial bodies express $P2X_3$ receptors. *Am. J. Respir. Cell Mol. Biol.* **23,** 52–61
33. Brouns, I., Oztay, F., Pintelon, I., De Proost, I., Lembrechts, R., Timmermans, J.-P., and Adriaensen, D. (2008) Neurochemical pattern of the complex innervation of neuroepithelial bodies in mouse lungs. *Histochem. Cell Biol.* doi: 10.1007/s00418–008-0495–7
34. De Proost, I., Pintelon, I., Brouns, I., Kroese, A. B. A., Riccardi, D., Kemp, P. J., Timmermans, J.-P., and Adriaensen, D. (2008) Functional live cell imaging of the pulmonary neuroepithelial body microenvironment. *Am. J. Respir. Cell Mol. Biol.* **39,** 180–189
35. Pintelon, I., De Proost, I., Brouns, I., Van Herck, H., Van Genechten, J., Van Meir, F., Timmermans, J.-P., and Adriaensen, D. (2005) Selective visualisation of neuroepithelial bodies in vibratome slices of living lung by 4-Di-2-ASP in various animal species. *Cell Tissue Res.* **321,** 21–33
36. Allen, T. G. J. (1997) The 'sniffer-patch' technique for detection of neurotransmitter release. *Trends. Neurosci.* **20,** 192–197
37. Taylor, S. C., and Peers, C. (2000) Three distinct Ca^{2+} influx pathways couple acetylcholine activation to catecholamine secretion from PC12 cells. *J. Neurochem.* **75,** 1583–1589
38. Bodin, P., and Burnstock, G. (2001) Purinergic signalling: ATP release. *Neurochem. Res.* **26,** 959–969
39. Aubrey, K. R., Rossi, F. M., Ruivo, R., Alboni, S., Bellenchi, G. C., Le Goff, A., Gasnier, B., and Supplisson, S. (2007) The transporters GlyT2 and VIAAT cooperate to determine the vesicular glycinergic phenotype. *J. Neurosci.* **27,** 6273–6281
40. Zhang, X., Chen, Y., Wang, C., and Huang, L.-Y. M. (2007) Neuronal somatic ATP release triggers neuron-satellite glial cell communication in dorsal root ganglia. *Proc. Natl. Acad. Sci. U. S. A.* **104,** 9864–9869
41. Silinsky, E. M., and Redman, R. S. (1996) Synchronous release of ATP and neurotransmitter within milliseconds of a motor nerve impulse in the frog. *J. Physiol.* **492,** 815–822
42. Brown, P., and Dale, N. (2002) Spike-independent release of ATP from Xenopus spinal neurons evoked by activation of glutamate receptors. *J. Physiol.* **540,** 851–860
43. Van Scott, M. R., Chinet, T. C., Burnette, A. D., and Paradiso, A. M. (1995) Purinergic regulation of ion transport across nonciliated bronchiolar epithelial (Clara) cells. *Am. J. Physiol.* **269,** L30–L37
44. Kishore, B. K., Ginns, S. M., Krane, C. M., Nielsen, S., and Knepper, M. A. (2000) Cellular localization of $P2Y_2$ purinoceptor in rat inner medulla and lung. *Am. J. Physiol. Renal. Physiol.* **278,** F43–F51
45. Fu, X. W., Nurse, C., and Cutz, E. (2004) Expression of functional purinergic receptors in pulmonary neuroepithelial bodies and their role in hypoxia chemotransmission. *Biol. Chem.* **385,** 275–284

Received for publication April 22, 2008.
Accepted for publication November 6, 2008.